Adaptive lenticular lens array using a hybrid liquid crystal–carbon nanotube nanophotonic device

Kanghee Won
Ranjith Rajasekharan
Philip Hands
Qing Dai
Timothy D. Wilkinson

Adaptive lenticular lens array using a hybrid liquid crystal–carbon nanotube nanophotonic device

Kanghee Won
Ranjith Rajasekharan
Philip Hands
Qing Dai
Timothy D. Wilkinson
University of Cambridge
Engineering Department
Electrical Engineering Division
9 JJ Thomson Avenue
Cambridge CB3 0FA, United Kingdom
E-mail: tdw13@cam.ac.uk

Abstract. We present a switchable liquid crystal cylindrical lens array fabricated with a combination of a sparse electrode array of multiwall carbon nanotubes (MWCNTs) grown upon a silicon substrate, and a second glass substrate featuring an in-plane switching (IPS) electrode structure. A cylindrical shape of an electric field profile was produced between the MWCNT substrate and the IPS substrate. This cylindrical shape was controlled by the application of an external electric field. The average focal lengths at different voltages were calculated. This adaptive lenticular lens array can be used in autostereoscopic displays. [DOI: 10.1117/1.3582172]

Subject terms: nanophotonic; carbon nanotube; liquid crystal; electro-optic device.

Paper 110058R received Jan. 19, 2011; revised manuscript received Mar. 25, 2011; accepted for publication Apr. 1, 2011; published online May 19, 2011.

1 Introduction

Three-dimensional (3D) displays are the current revolution in display technology, and many autostereoscopic techniques have been introduced.[1,2] Among them, the lenticular lens array is widely used in specialist applications of electronic displays. A lenticular lens is an array of cylindrical and magnifying lenses. The images viewed from different angles make the images that appear to change or move. A switchable lenticular lens array could be a suitable candidate, to be included in 3D displays without glasses. However, the device performance of lenticular lens arrays is often limited by low image quality and inaccurate focal length caused by spherical aberration. This limitation causes the lenticular lens array to be generally fixed and the focal length in conjunction with the image is not easily changed.

The objective of this paper is to outline an adaptive lenticular lens array model in order to significantly improve image quality, and to develop an enhanced fabrication technology for the adaptive lenticular lens array.[3–9]

2 Experimental

The carbon nanotube (CNT) array was fabricated using plasma enhanced chemical vapor deposition. E-beam lithography and sputter-coating processes were employed to pattern nickel dot islands with 100 nm diameter and 10 μm periodicity. The silicon substrate was then placed inside a vacuum chamber and heated to 650°C. Ammonia gas was then introduced into the chamber to etch the surface of the nickel catalyst islands. Acetylene was used as a carbon source, and was released into the chamber after the temperature reached 690°C. A dc voltage of 640 V was then also applied to create a plasma. The growth process lasted for 15 min at 720°C, which gave multiwall carbon nanotubes (MWCNTs) of nearly 2 μm in height (Fig. 1).

The second substrate of the liquid crystal CNT (LC-CNT) cell consisted of a patterned indium tin oxide (ITO)- coated glass substrate. The ITO was patterned using photolithography to give two inter- digitated electrodes with an in-plane switching (IPS) structure. These two electrodes are denoted as pixel (source) electrode and common (counter) electrode. Figure 2(a) shows the structure of the IPS cell employed in this study. The electrode width is 4 μm and the electrode spacing is 10 μm.

The MWCNTs of 50 nm in diameter and 2 μm in height were patterned on the lower substrate with a 10 μm spacing between the nanotubes as shown in Fig. 2(b). Potential differences of between 0 V and 8 V_{rms} were applied between the MWCNT array and the common electrode, while the pixel electrode was set to ground (0 V).

A polyimide (AM4276 from Merck) was applied to the upper substrate for a homogeneous planar LC alignment, which yields a low pretilt angle of 2 deg after rubbing. The upper and lower substrates were separated with a uniform gap of 20 μm, defined by spacer beads mixed into UV-curing adhesive. A positive dielectric anisotropy nematic LC mixture (BL048, Merck, Merck, Germany) was filled into the cell by capillary action. The material parameters of BL048 are listed as follows: birefringence, $\triangle n = 0.226$ at $\lambda = 523$ nm; dielectric anisotropy, $\triangle\varepsilon = 16.8$; elastic constants, $K_{11} = 15.5$ pN, $K_{22} = 12$ pN, $K_{33} = 28$ pN, and rotational viscosity $\gamma_1 = 0.047$ Pa s (see Fig. 3).

The lens properties were observed by an interferometric method,[6] and worked in reflective mode in conjunction with an optical microscope. The LC-CNT cell was placed between two crossed polarizers while the cell rubbing direction oriented was at 45° with respect to the polarizer. A He–Ne laser beam ($\lambda = 0.633$ μm) along with a beam expander used as the light source and the interference patterns were captured by a CCD camera with frame grabber. A voltage source was used to observe the variation of interference fringes with various values of potential difference.

3 Results and Discussion

When there was no electric field applied, the liquid crystal molecules aligned parallel to the upper (IPS) substrate (and parallel to the IPS electrodes) due to the rubbed polyimide alignment layer. However, a defect in the LC director was visible surrounding the MWCNTs [shown in Fig. 4(a)]. Previous work has shown that when a voltage is applied, the field profile from the MWCNTs to the opposite electrode

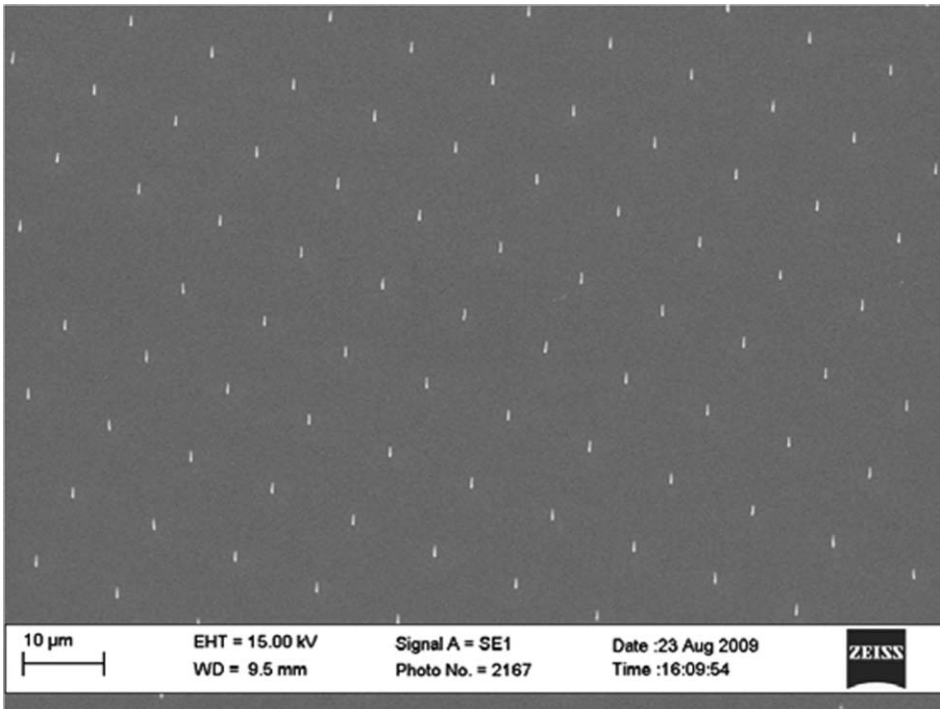

Fig. 1 Scanning electron microscope image of single nanotube electrode on silicon substrate.

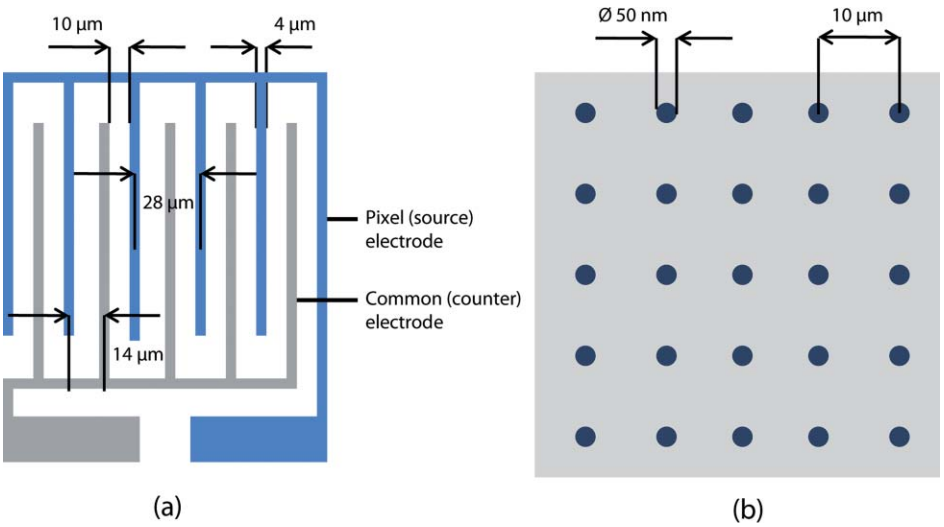

Fig. 2 Structure of (a) IPS electrode, and (b) MWCNT array substrate.

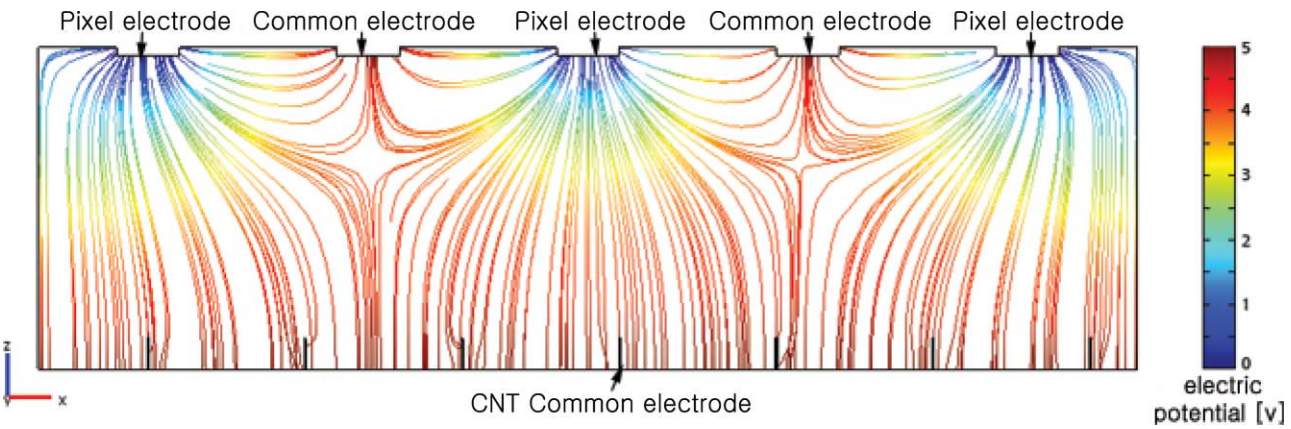

Fig. 3 Simulated electrical field profile of device with an applied field of 5 V μm^{-1}.

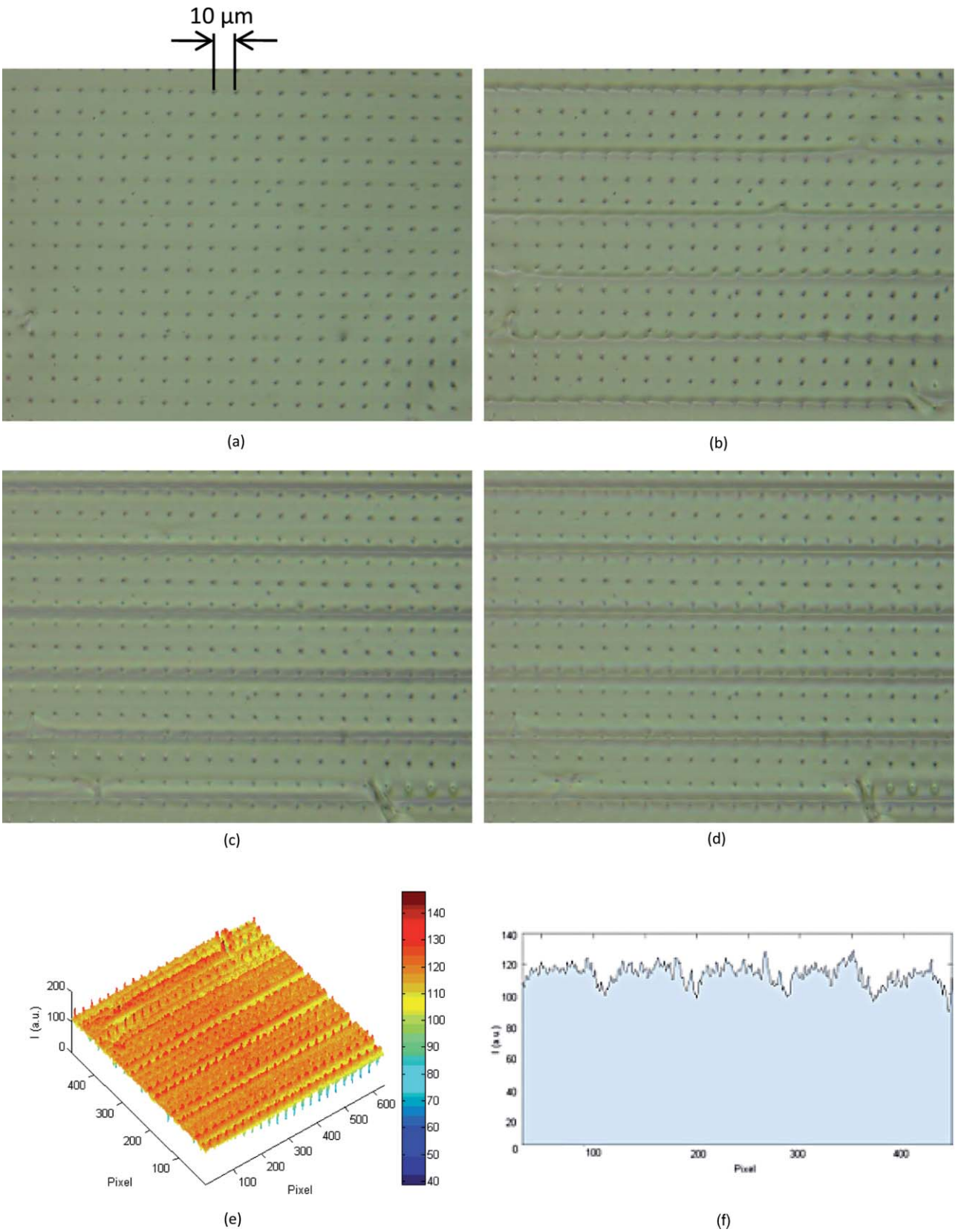

Fig. 4 Optical microscopic images of device switching at four different voltages: (a) 0, (b) 2, (c) 3, and (d) 4 V_{rms}. Intensity profile (e), and Cross-sectional profile (f) of the liquid crystal lens array switching at 3 V_{rms}.

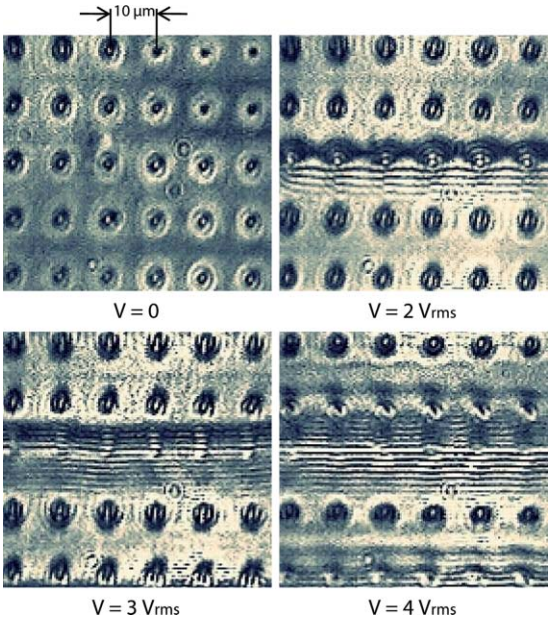

Fig. 5 Interference fringe patterns at various values of applied voltage.

is approximately Gaussian-shaped,[10] due to strong localized field enhancements. By placing nanotubes at 10 μm separation, the Gaussian electric field profile from each nanotube site further distorts the in-plane electric field generated between IPS electrodes. This results in a stronger lensing effect than would be achieved without the MWCNTs. The resulting field profile is highly complex, but is approximately cylindrical in shape. A cross section of the device was simulated using COMSOL Multiphysics, and is shown in Fig. 3. for an applied potential of 5 V between source and common electrodes.

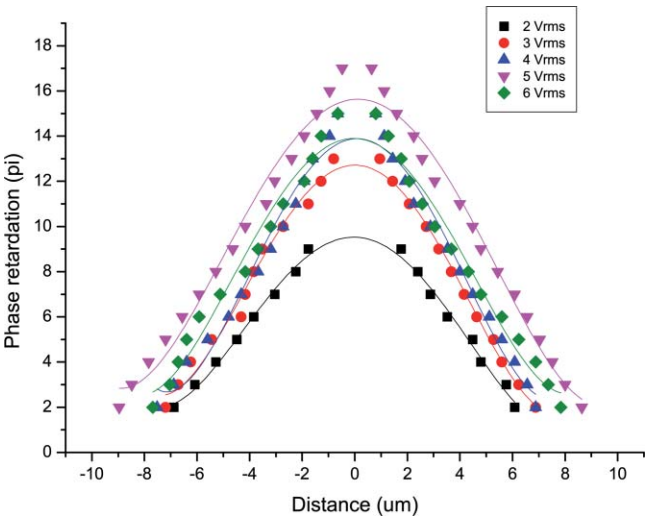

Fig. 6 Phase profiles at different applied voltages.

Experimental results for the images of device switching at different operating voltages are shown in Figs. 4(a)–4(d). A CCD camera was used for recording the images using reflected light microscopy. Also, a representative intensity profile in the x-y plane and a cross-sectional profile cut perpendicular to the pattern are shown in Figs. 4(e) and 4(f).

The fringe patterns in Fig. 5 are generated due to the modulation of the liquid crystal refractive index with applied voltage. The corresponding graded retardance results in a modulation in transmitted light intensity through the crossed polarizers.[11]

Figure 5 shows the observed fringe patterns when various values of potential difference were applied across the cell. The fringe patterns are composed of nearly straight parallel lines, and the phase difference between two adjacent lines is 2π radians. The first interference fringe was observed at

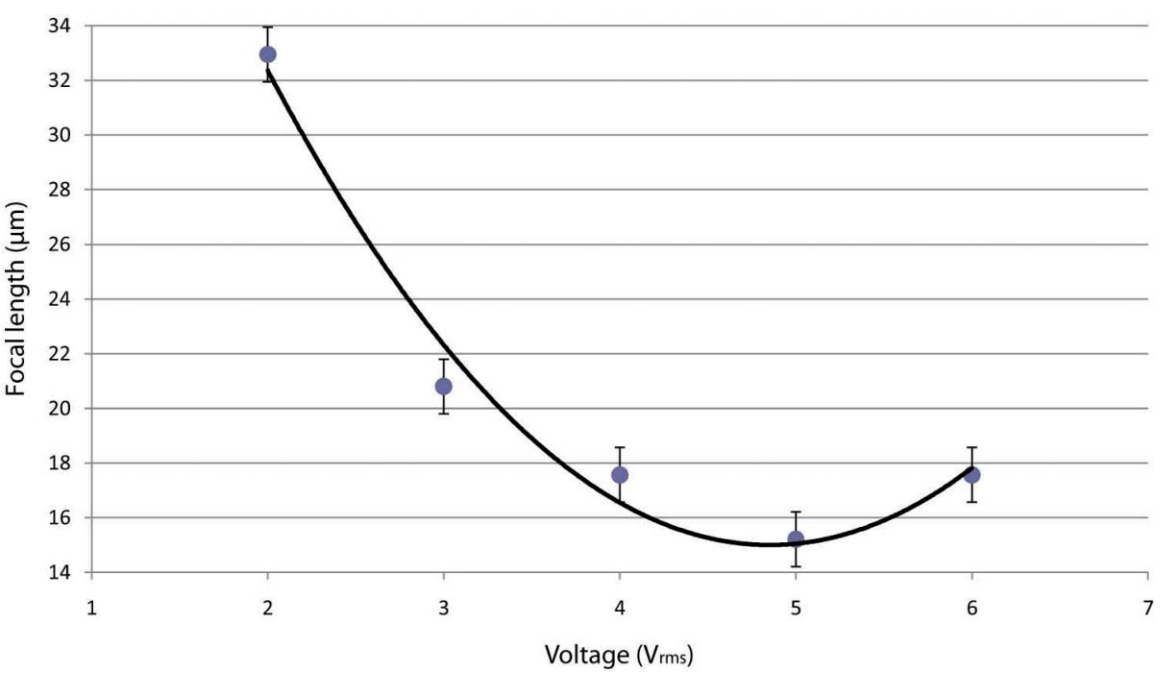

Fig. 7 Focal length variation with respect to external voltage. The solid line acts as a guide for the eyes only.

2 V_{rms} and more begin to appear from the centre outwards with higher applied voltages. The number of the interference fringes was greatest with 5 V_{rms}, beyond which the number of fringes decreased gradually.

The average phase retardation profile across the fringes was then calculated and is plotted in Fig. 6 for several different applied voltages. The phase profile is similar in shape to a lens with positive focal length. The trendlines in Fig. 6 show 4th order polynomial function fits for the phase profile, and are shown as a guide for the eyes only. Furthermore, as the different voltages were applied across the cell, wide ranges of focal lengths were observed because the refractive index difference across the lens aperture was altered by the E-field profile.[12,13]

From Fresnel's approximation,[14–16] the focal length of a cylindrical LC lens can be estimated as:

$$f = \frac{\pi w^2}{4\lambda\Delta\delta}$$

where w is the aperture width, $\Delta\delta$ is the phase delay between the center and edge of the aperture, and λ is the wavelength. The data in Fig. 6 can therefore be used to calculate an approximation of the focal length for each applied voltage. This data is presented in Fig. 7.

At $V = 0$, the LC-CNT lens cell exhibits a homogeneous planar LC alignment due to the surface anchoring effect from the top substrate. Thus, no focusing effect occurs ($f = \infty$) until the Freedrickzs transition is passed. The first fringes (and measurable focal length) were seen at 2 V_{rms}. The focal length of the LC device then decreases with increasing applied voltage.

The shortest focal length was approximately 15.2 ($\pm$ 1.0) μm at a voltage of 5 V_{rms}. As the voltage increased further from 5 to 6 V_{rms}, a slight increase in the focal length is observed. For voltages above 7 V_{rms} the LC became distorted, and interference fringe patterns were not investigated.

4 Conclusion

In conclusion, we demonstrate a two-voltage-driven adaptive LC cylindrical lens array made from a hybrid MWCNT array and patterned in-plane-switching electrodes. The resulting electric field profile within the device was first simulated and was found to give a profile that approximated an array of cylindrical lenses. Its phase retardation was then quantified experimentally using an interferometric technique, and results confirmed the predicted cylindrical lens phase retardation profile. Additionally, the voltage-dependent focal length of the lenticular lens array was calculated and was found to switch from $f = \infty$ to approximately 15.2 μm. This performance could be improved further by use of higher birefringence LCs. Such electrically variable lenses might therefore be considered candidates for ways of making an adaptive lenticular lens array for autostereopic displays.

References

1. J.-Y. Son, V. V. Saveljev, Y.-J. Choi, J.-E. Bahn, S.-K. Kim, and H. Choi, "Parameters for designing autostereoscopic imaging systems based on lenticular, parallax barrier, and integral photography plates," *Opt. Eng.* **42**(11), 3326–3333 (2003).
2. S. Pastoor and M. Wopking, "3-D displays: A review of current technologies," *Displays* **17**(2), 100–110 (1997).
3. S. T. Kowel, P. Kornreich, and A. Nouhi, "Adaptive spherical lens," *Appl. Opt.* **23**(16), 2774–2777 (1984).
4. N. A. Riza, and M. C. Dejule, "3-Terminal adaptive nematic liquid-crystal lens device," *Opt. Lett.* **19**(14), 1013–1015 (1994).
5. A. F. Naumov, M. Yu. Loktev, I. R. Guralnik, and G. Vdovin, "Liquid-crystal adaptive lenses with modal control," *Opt. Lett.* **23**(13), 992–994 (1998).
6. R. Rajasekharan-Unnithan, H. Butt, and T. D. Wilkinson, "Optical phase modulation using a hybrid carbon nanotube-liquid-crystal nanophotonic device," *Opt. Lett.* **34**(8), 1237–1239 (2009).
7. M. Ye and S. Sato, "Optical properties of liquid crystal lens of any size," *Jpn. J. Appl. Phys., Part 2* **41**(5B), L571–L573 (2002).
8. X. Wang, T. D. Wilkinson, M. Mann, K. B. K. Teo, and W. I. Milne, "Characterization of a liquid crystal microlens array using multi-walled carbon nanotube electrodes," *Appl. Opt.* **49**(17), 3311–3315 (2010).
9. S. Sato, "Liquid-crystal lens-cells with variable focal length," *Jpn. J. Appl. Phys.* **18**(9), 1679–1684 (1979).
10. T. D. Wilkinson, X. Wang, K. B. K. Teo, and W. I. Milne, "Sparse multiwall carbon nanotube electrode arrays for liquid-crystal photonic devices," *Adv. Mater.* **20**(2), 363–366 (2008).
11. M. Ye, Y. Yokoyama, and S. Sato, "Liquid crystal lens prepared utilizing patterned molecular orientations on cell walls," *Appl. Phys. Lett.* **89**, 141112 (2006).
12. M. Ye, B. Wang, M. Yamaguchi, and S. Sato, "Reducing driving voltages for liquid crystal lens using weakly conductive thin film," *Jpn. J. Appl. Phys.* **47**(6), 4597–4599 (2008).
13. M. Ye, B. Wang, M. Kawamura, and S. Sato, "Fast switching between negative and positive power of liquid crystal lens," *Electron. Lett.* **43**(8), 474–476 (2007).
14. E. Hecht, *Optics*, Addison Wesley, San Francisco, London (2002).
15. O. A. Zayakin, M. Y. Loktev, G. D. Love et al., "Cylindrical adaptive lenses," *Sixth International Symposium on Atmospheric and Ocean Optics*, **3983**, 112–117, Proc. SPIE, Tomsk, Russia (1999).
16. H. W. Ren, Y. H. Fan, S. Gauza, and S.-T. Wu, "Tunable-focus cylindrical liquid crystal lens," *Jpn. J. Appl. Phys., Part 1* **43**(2), 652–653 (2004).

Kanghee Won obtained his mphil in industrial Systems, Manufacturing and Management at the University of Cambridge. After completing his MS degree, he joined the CMMPE group in October 2008 for a PhD, and he is currently working on hybrid liquid crystal–carbon nanotube devices, focusing on understanding how these electro-optical devices work with LCs, and finding the optimal device configuration for various applications.

Ranjith Rajasekharan obtained his MS degree from Cochin University of Science and Technology, India. He then worked for the Indian Space Research Organization as a scientist/engineer before coming to Cambridge for a PhD in 2007. His area of interest is in the development of novel electro-optic sensors.

Philip Hands has an MSci in physics (1999) and a PhD in condensed matter physics (2003), both from Durham University. His PhD studied the quantum tunneling conduction mechanisms in metal-polymer composites and their applications in array-based chemical vapor sensing (electronic noses). He also has postdoctoral experience at the Center for Advanced Instrumentation, Durham University, in the fabrication and applications of adaptive liquid crystal devices. In particular he developed adaptive lenses for applications in 3D displays, optical tweezing and adaptive optics for astronomy. He is currently employed on the COSMOS project, developing the performance and applications of chiral nematic liquid crystal lasers.

Qing Dai graduated from Imperial College, London with an MEng in electronic and electrical Engineering (2007). In 2008 he joined the CMMPE group as a PhD student, and his research is concerned with applications of carbon nanotubes, especially for liquid-crystal photonic devices.

Timothy D. Wilkinson received his undergraduate degree from Canterbury University, New Zealand, and his PhD degree from Magdalene College, Cambridge, in 1994. He is currently a reader in photonic engineering in the engineering department of Cambridge University and a fellow of Jesus College. He has been working in the field of photonics, devices, and systems for more than 19 years. His current research has been in applications of holographic technology. This includes new liquid crystal device structures based on sparse arrays of vertically grown multiwall carbon nanotubes, where the tubes are used as tiny electrodes to great 3-D electric field profiles and graded refractive index structures, which may have applications such as switchable lenslet arrays and 3-D displays.